Study of the scalar and pseudoscalar meson mass spectrum of QCD above the chiral transition, using an effective Lagrangian approach

Giulio Cianti
giulio.cianti@uniroma1.it
Cortona
22/05/2025

QCD describes the strong interactions between quarks and gluons.

It is an $SU(N_c)$ gauge theory with $\boldsymbol{N_c = 3}$ **colors** and a matter content of $\boldsymbol{N_f = 6}$ **quark flavors**. The fundamental fields of the theory are:

- **Gluons**: $A_\mu = A_\mu^a T_a, \quad a = 1, \dots, N_c^2 - 1 = 8$;
- **Quarks**: $\psi_{f,i}, \quad f = 1, \dots, N_f;\ i = 1, \dots, N_c$.

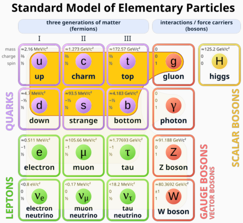

Figure 1: Elementary particles of the SM.

The **QCD Lagrangian** combines these fields as follows:

$$\mathscr{L}_{QCD} = -\frac{1}{2}\mathrm{Tr}\left[F_{\mu\nu}F^{\mu\nu}\right] + \overline{\psi}_f\left[i\gamma^\mu D_\mu - m_f\right]\psi_f .$$

- $D_\mu = \partial_\mu + igA_\mu$ is the covariant derivative;
- $F_{\mu\nu} = \partial_\mu A_\nu - \partial_\nu A_\mu + ig\left[A_\mu, A_\nu\right]$ is the field strength tensor.

QCD: properties & approaches

1. **Asymptotic freedom**: At high energies, the renormalized coupling constant g_R goes to zero;
2. **Infrared slavery**: At low energies, g_R grows, making perturbation theory unreliable;

$\Rightarrow$ **Non-perturbative methods** are needed to study QCD at low energies:

- **Lattice QCD**: provides regularization and a continuum limit corresponding to a weakly coupled regime of the theory.
- **Effective Lagrangian models**: capture low-energy dynamics by emphasizing the theory's symmetry structure.

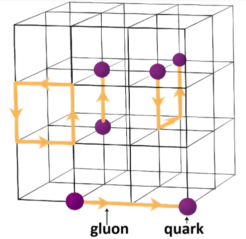

Figure 2: Visual representation of the lattice discretization.

Chiral symmetry

In the **chiral limit** of N_f massless quarks, $\mathscr{L}_{QCD}$ is invariant under the **flavor chiral group** $G = U(N_f)_L \otimes U(N_f)_R$:

$$\psi = \begin{pmatrix} \psi_L \\ \psi_R \end{pmatrix} \to \psi' = \begin{pmatrix} \psi'_L = V_L \psi_L \\ \psi'_R = V_R \psi_R \end{pmatrix}, \qquad V_{L,R} \in U(N_f).$$

These decompose into vectorial ($V_L = V_R \equiv V$) and axial transformations ($V_L = V_R^{-1} \equiv A$):

$$\boldsymbol{G = U(1)_V \otimes SU(N_f)_V \otimes U(1)_A \otimes SU(N_f)_A.}$$

The physically relevant cases are the following:

- $\boldsymbol{N_f = 2}$ ($m_{u,d} = 0$), extension of $SU(2)_V$ isospin symmetry;
- $\boldsymbol{N_f = 3}$ ($m_{u,d,s} = 0$), extension of $SU(3)_V$ Gell-Mann symmetry;
- **"ideal"** $\boldsymbol{N_f = 2 + 1}$ ($m_{u,d} = 0$, $m_s \neq 0$);
- **"realistic"** $\boldsymbol{N_f = 2 + 1}$ with exact isospin symmetry ($0 < m_{u,d} \equiv m_l \ll m_s$).

Chiral symmetry breaking and restoration

$\boldsymbol{U(1)_V}$ is **exactly realized** (i.e., baryon number conservation).

Special unitary part is **spontaneously broken**:

$$\boldsymbol{SU(N_f)_V \otimes SU(N_f)_A \rightarrow SU(N_f)_V},$$

$\Rightarrow$ $N_f^2 - 1$ Goldstone bosons: pion triplet for $N_f = 2$, pseudoscalar octet for $N_f = 3$;

$\Rightarrow$ Order parameter: **chiral condensate** $\boldsymbol{\Sigma = \langle \overline{\psi}\psi \rangle \neq 0}$.

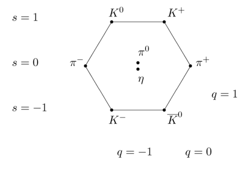

Figure 3: Pseudoscalar octet.

At finite T:

$$\Sigma = \langle \overline{\psi}\psi \rangle = \frac{\mathrm{Tr}\big[e^{-\beta H}\overline{\psi}\psi\big]}{\mathrm{Tr}\big[e^{-\beta H}\big]}.$$

In the chiral limit, Σ vanishes for $T > T_c^{(N_f)}$ (**chiral transition**).

With explicit symmetry breaking, there is a **chiral crossover**.
The **pseudocritical temperature** for this chiral crossover, computed in [Bazavov et al., 2019a], is $T_{pc} = 156.5 \pm 1.5$ MeV.

The fate of $U(1)_A$ symmetry

In the chiral limit, the Noether current J_5^μ is anomalous: $\partial_\mu J_5^\mu = 2N_f \mathcal{Q}$, with $\mathcal{Q} \equiv \frac{g^2}{16\pi^2}\mathrm{Tr}\left[F^{\mu\nu}\widetilde{F}_{\mu\nu}\right]$ the topological charge density.

$\implies$ $\boldsymbol{U(1)_A}$ symmetry **anomalously broken**.

At finite temperature:

- For $T < T_c^{(N_f)}$, Σ acts also as an order parameter for $U(1)_A$.
- For $T \geq T_c^{(N_f)}$, the anomaly persists, but the topologically non-trivial gauge field configurations are thermally suppressed.
  $\implies$ $U(1)_A$ may be **effectively restored** above $\boldsymbol{T_{U(1)} > T_c^{(N_f)}}$.

Whether $\boldsymbol{T_{U(1)} \gg T_c^{(N_f)}}$ or $\boldsymbol{T_{U(1)} \gtrsim T_c^{(N_f)}}$ is relevant for the **order of the chiral phase transition**.

Chiral Effective Lagrangian

The effective theory of QCD at $T = 0$ is the **Chiral Effective Theory**:

$$\mathscr{L}_{eff} = \frac{1}{2}\mathrm{Tr}\left[\partial_\mu U \partial^\mu U^\dagger\right] + \frac{B_m}{2\sqrt{2}}\mathrm{Tr}\left[\mathbf{M}U + \mathbf{M}^\dagger U^\dagger\right],$$

with U the $N_f \times N_f$ **meson matrix field** and $\mathbf{M} = \mathrm{diag}(m_1, \ldots, m_{N_f})$ the quark mass matrix (no CP-violation).
The first term is invariant under $\boldsymbol{G : U \to V_L U V_R^{-1}}$, the second one introduces explicit chiral symmetry breaking.

This theory omits key **degrees of freedom** relevant near the chiral transition:

- The **pseudoscalar singlet** from $U(1)_A$;
- The **scalar partners** of pseudoscalar mesons.

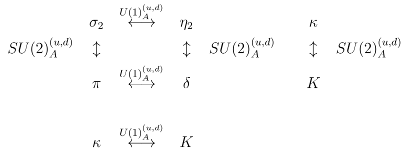

Figure 4: Operator degeneracies from $SU(N_f)_A$ and $U(1)_A$ transformations.

Extended linear sigma (EL_σ) model

The EL_σ model is an effective model with N_f^2 pseudoscalar and N_f^2 scalar fields, with a term that mimics the axial anomaly.

Lagrangian: $$\mathscr{L}_{(EL_\sigma)}(U, U^\dagger) = \frac{1}{2}\mathrm{Tr}\left[\partial_\mu U \partial^\mu U^\dagger\right] - V(U, U^\dagger).$$

Potential: $$V(U, U^\dagger) = \frac{1}{4}\lambda_\pi^2 \mathrm{Tr}\left[(UU^\dagger - \rho_\pi \mathbb{1})^2\right] + \frac{1}{4}\lambda_\pi'^2 \mathrm{Tr}\left[UU^\dagger\right]^2 + \\ - \frac{B_m}{2\sqrt{2}}\mathrm{Tr}\left[\mathbf{M}U + \mathbf{M}^\dagger U^\dagger\right] - k\left[\det U + \det U^\dagger\right].$$

- $\mathscr{L}_{(EL_\sigma)}\Big|_{\mathbf{M}=0}$ is invariant under $U(1)_V \otimes SU(N_f)_V \otimes SU(N_f)_A$;
- $U(1)_A$ is explicitly broken by the **anomalous term** ($G : U \to V_L U V_R^{-1}$, $\det U \to e^{2iN_f\alpha_A} \det U$);
- T dependence is encoded in the **parameters** $\{\lambda_\pi, \rho_\pi, \lambda_\pi', B_m, k\}$.

Predictions of the model: stationary point

Building upon [Meggiolaro and Mordà, 2013] and [Meggiolaro, 2023], we take $\mathbf{M} = \mathrm{diag}(m_l, m_l, m_s)$ and minimize $V(U, U^\dagger)$ for $\boldsymbol{T > T_c^{(N_f)}}$.

Parametrization: $U = \begin{bmatrix} \frac{\sigma_2+\delta^0}{\sqrt{2}} + i\frac{\eta_2+\pi^0}{\sqrt{2}} & \delta^+ + i\pi^+ & \kappa^+ + iK^+ \\ \delta^- + i\pi^- & \frac{\sigma_2-\delta^0}{\sqrt{2}} + i\frac{\eta_2-\pi^0}{\sqrt{2}} & \kappa^0 + iK^0 \\ \kappa^- + iK^- & \bar{\kappa}^0 + i\bar{K}^0 & \sigma_s + i\eta_s \end{bmatrix}$;

Residual symmetries: P, $SU(2)_V^{(u,d)} \Longrightarrow \begin{cases} \langle\pi\rangle = \langle K\rangle = \langle\eta\rangle = 0 \\ \langle\delta\rangle = \langle\kappa\rangle = 0 \end{cases}$;

Matrix field vev: $\overline{U} = \begin{bmatrix} \frac{\bar{\sigma}_2}{\sqrt{2}} & 0 & 0 \\ 0 & \frac{\bar{\sigma}_2}{\sqrt{2}} & 0 \\ 0 & 0 & \bar{\sigma}_s \end{bmatrix}$;

Predictions of the model: stationary point

Building upon [Meggiolaro and Mordà, 2013] and [Meggiolaro, 2023], we take $\mathbf{M} = \mathrm{diag}(m_l, m_l, m_s)$ and minimize $V(U, U^\dagger)$ for $\boldsymbol{T > T_c^{(N_f)}}$.

Matrix field vev: $$\overline{U} = \begin{bmatrix} \frac{\bar{\sigma}_2}{\sqrt{2}} & 0 & 0 \\ 0 & \frac{\bar{\sigma}_2}{\sqrt{2}} & 0 \\ 0 & 0 & \bar{\sigma}_s \end{bmatrix};$$

$$\langle \overline{\psi}_l \psi_l \rangle = \langle \overline{\psi}_u \psi_u \rangle + \langle \overline{\psi}_d \psi_d \rangle = \frac{\partial \overline{V}}{\partial m_l} = -B_m \bar{\sigma}_2, \quad \langle \overline{\psi}_s \psi_s \rangle = \frac{\partial \overline{V}}{\partial m_s} = -\frac{B_m}{\sqrt{2}} \bar{\sigma}_s;$$

Stationary-point (SP) condition:

$$\begin{cases} (\lambda_\pi^2 + \lambda_\pi'^2)\bar{\sigma}_s^3 + (\lambda_\pi'^2 \bar{\sigma}_2^2 - \lambda_\pi^2 \rho_\pi)\bar{\sigma}_s - \frac{B_m}{\sqrt{2}} m_s - k\bar{\sigma}_2^2 = 0 \\ \left(\frac{1}{2}\lambda_\pi^2 + \lambda_\pi'^2\right)\bar{\sigma}_2^3 + \left(\lambda_\pi'^2 \bar{\sigma}_s^2 - \lambda_\pi^2 \rho_\pi - 2k\bar{\sigma}_s\right)\bar{\sigma}_2 - B_m m_l = 0 \end{cases} .$$

Predictions of the model: meson mass spectrum

Computing and diagonalizing the Hessian matrix, we find the **meson mass spectrum** of the theory in terms of Lagrangian parameters and vevs $\left(\tilde{\rho}_\pi \equiv \rho_\pi - \frac{\lambda_\pi'^2}{\lambda_\pi^2}\left(\bar{\sigma}_s^2 + \bar{\sigma}_2^2\right)\right)$:

$$M_\pi^2 = -\lambda_\pi^2\tilde{\rho}_\pi + \frac{1}{2}\lambda_\pi^2\bar{\sigma}_2^2 - 2k\bar{\sigma}_s; \qquad M_\delta^2 = -\lambda_\pi^2\tilde{\rho}_\pi + \frac{3}{2}\lambda_\pi^2\bar{\sigma}_2^2 + 2k\bar{\sigma}_s;$$

$$M_K^2 = -\lambda_\pi^2\tilde{\rho}_\pi + \lambda_\pi^2\left(\frac{\bar{\sigma}_2^2}{2} + \bar{\sigma}_s^2\right) - \frac{1}{\sqrt{2}}\left(\lambda_\pi^2\bar{\sigma}_s + 2k\right)\bar{\sigma}_2;$$

$$M_\kappa^2 = -\lambda_\pi^2\tilde{\rho}_\pi + \lambda_\pi^2\left(\frac{\bar{\sigma}_2^2}{2} + \bar{\sigma}_s^2\right) + \frac{1}{\sqrt{2}}\left(\lambda_\pi^2\bar{\sigma}_s + 2k\right)\bar{\sigma}_2;$$

$$M_{\eta_l,\eta_h}^2 = -\lambda_\pi^2\tilde{\rho}_\pi + \frac{\lambda_\pi^2}{2}\left(\frac{\bar{\sigma}_2^2}{2} + \bar{\sigma}_s^2\right) + k\bar{\sigma}_s \mp \sqrt{\left(\frac{\lambda_\pi^2}{2}\left(\frac{\bar{\sigma}_2^2}{2} - \bar{\sigma}_s^2\right) + k\bar{\sigma}_s\right)^2 + 4k^2\bar{\sigma}_2^2};$$

$$M_{\sigma_l,\sigma_h}^2 = -\lambda_\pi^2\tilde{\rho}_\pi + \frac{3\lambda_\pi^2}{2}\left(\frac{\bar{\sigma}_2^2}{2} + \bar{\sigma}_s^2\right) + \lambda_\pi'^2\left(\bar{\sigma}_2^2 + \bar{\sigma}_s^2\right) - k\bar{\sigma}_s +$$

$$\mp \sqrt{\left[\frac{3\lambda_\pi^2}{2}\left(\frac{\bar{\sigma}_2^2}{2} - \bar{\sigma}_s^2\right) + \lambda_\pi'^2\left(\bar{\sigma}_2^2 - \bar{\sigma}_s^2\right) + k\bar{\sigma}_s\right]^2 + 4\bar{\sigma}_2^2\left(\lambda_\pi'^2\bar{\sigma}_s - k\right)^2}.$$

Comparison with the lattice data

From [Bazavov et al., 2019b] we get the meson masses M_π, M_δ, M_K and M_κ, but we are more interested in the **meson mass splittings**:

$$\Delta_{\delta\pi} \equiv M_\delta^2 - M_\pi^2 = \lambda_\pi^2 \bar{\sigma}_2^2 + 4k\bar{\sigma}_s;$$
$$\Delta_{K\pi} \equiv M_K^2 - M_\pi^2 = (\lambda_\pi^2 \bar{\sigma}_s + 2k)\left(\bar{\sigma}_s - \frac{\bar{\sigma}_2}{\sqrt{2}}\right);$$
$$\Delta_{\kappa K} \equiv M_\kappa^2 - M_K^2 = \sqrt{2}(\lambda_\pi^2 \bar{\sigma}_s + 2k)\bar{\sigma}_2 = \sqrt{2}\lambda_\pi^2 \bar{\sigma}_s \bar{\sigma}_2 + 2\sqrt{2}k\bar{\sigma}_2.$$

From these splittings, we obtain a relation that links the two vevs mentioned before:

$$\bar{\sigma}_s = \left(2\frac{\Delta_{K\pi}}{\Delta_{\kappa K}} + 1\right)\frac{\bar{\sigma}_2}{\sqrt{2}} \equiv m' \frac{\bar{\sigma}_2}{\sqrt{2}},$$

which can be used to extrapolate the value of some **combinations of Lagrangian parameters and vevs** in terms of **lattice data**.

Comparison with the lattice data: $k\bar{\sigma}_2$ and $k\bar{\sigma}_s$

$$k\bar{\sigma}_2 = \frac{1}{2\sqrt{2}}\frac{m'}{(m')^2-1}\left(\Delta_{\delta\pi} - \frac{\Delta_{\kappa K}}{m'}\right).$$

$$k\bar{\sigma}_s = \frac{1}{2\sqrt{2}}\frac{(m')^2}{(m')^2-1}\left(\Delta_{\delta\pi} - \frac{\Delta_{\kappa K}}{m'}\right).$$

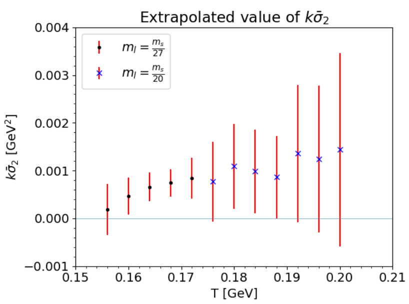

Figure 5: Extrapolated value of $k\bar{\sigma}_2$.

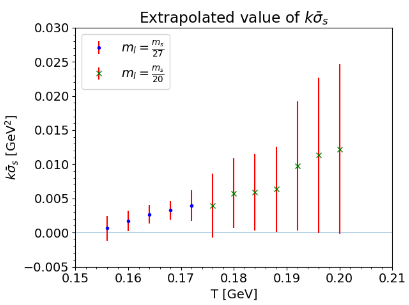

Figure 6: Extrapolated value of $k\bar{\sigma}_s$.

Comparison with the lattice data: meson mass splitting

$$\Delta_{\kappa K} = \sqrt{2}\lambda_\pi^2 \bar{\sigma}_s \bar{\sigma}_2 + 2\sqrt{2} k \bar{\sigma}_2.$$

$$\Delta_{\delta\pi} = \lambda_\pi^2 \bar{\sigma}_2^2 + 4k\bar{\sigma}_s.$$

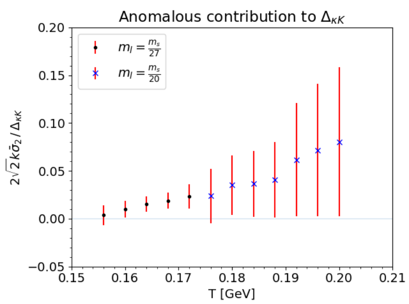

Figure 7: Anomalous contributions to $\Delta_{\kappa K}$.

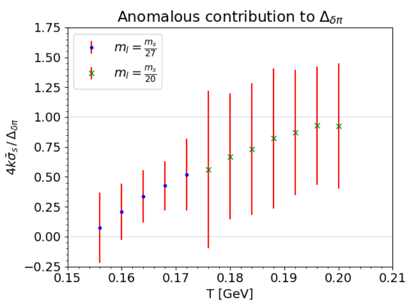

Figure 8: Anomalous contributions to $\Delta_{\delta\pi}$.

The model predicts a relation between scalar and pseudoscalar meson masses:

$$\frac{M_\kappa}{M_K} = \sqrt{\frac{\frac{m_s}{m_l} - 1}{\left(\frac{m_s}{m_l} + 1\right)\left(\frac{M_\pi}{M_K}\right)^2 - 2}}\,\frac{M_\pi}{M_K}.$$

As T increases and $M_\pi \approx M_K$, the scalar kaon mass also tends to become degenerate.

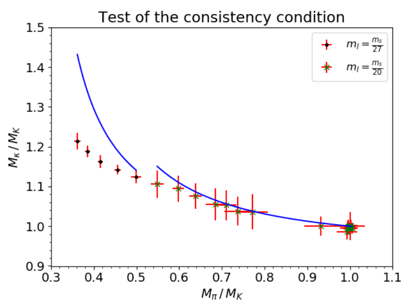

Figure 9: Lattice data compared with model's predictions. T increases left to right starting from T_{pc}.

Conclusions

1. A valid solution of the EL_σ model in the "realistic" $N_f = 2+1$ case with exact $SU(2)_V^{(u,d)}$ isospin symmetry exists for $\boldsymbol{T} > \boldsymbol{T_{pc}}$;
2. The quantities $\boldsymbol{k\bar{\sigma}_2}$ and $\boldsymbol{k\bar{\sigma}_s}$ can be considered **incompatible with zero** for $\boldsymbol{T} \gtrsim \boldsymbol{T_{pc}}$:
   - $\Rightarrow$ Evidence that $\boldsymbol{k} \neq \mathbf{0}$ above the transition;
   - $\Rightarrow$ $\boldsymbol{U(1)_A}$ **symmetry manifestly broken above the chiral transition**;
3. The contribution from the **anomalous term** is negligible for $\Delta_{\kappa K}$, but **highly significant** for $\boldsymbol{\Delta_{\delta\pi}}$;
4. The **predictions** of the model are **qualitatively compatible** with lattice data, but there are notable incompatibilities.

Thank you for your attention!

References i

[Bazavov et al., 2019a] Bazavov, A. et al. (2019a). **Chiral crossover in QCD at zero and non-zero chemical potentials.** *Phys. Lett. B*, 795:15–21.

[Bazavov et al., 2019b] Bazavov, A. et al. (2019b). **Meson screening masses in (2+1)-flavor QCD.** *Phys. Rev. D*, 100(9):094510.

[Ding et al., 2019] Ding, H. T. et al. (2019). **Chiral Phase Transition Temperature in (2+1)-Flavor QCD.** *Phys. Rev. Lett.*, 123(6):062002.

[Meggiolaro, 2023] Meggiolaro, E. (2023). **Study (using a chiral effective Lagrangian model) of the scalar and pseudoscalar meson mass spectrum of QCD at finite temperature, above T_c.** arXiv:2310.10339 [hep-ph].

[Meggiolaro and Mordà, 2013] Meggiolaro, E. and Mordà, A. (2013). **Remarks on the $U(1)$ axial symmetry and the chiral transition in QCD at finite temperature.** *Phys. Rev. D*, 88(9):096010.

[Navas et al., 2024] Navas, S. et al. (2024). **Review of particle physics.** *Phys. Rev. D*, 110(3):030001.

[Xu et al., 2023] Xu, Y.-Z., Qin, S.-X., and Zong, H.-S. (2023). **Chiral symmetry restoration and properties of Goldstone bosons at finite temperature*.** *Chin. Phys. C*, 47(3):033107.

Predictions of the model: stationary point

The first SP condition can be rewritten as a **constraint** for $\bar{\sigma}_s$:

$$\bar{\sigma}_2^2 = \frac{1}{k - \lambda_\pi'^2 \bar{\sigma}_s}\left[(\lambda_\pi^2 + \lambda_\pi'^2)\bar{\sigma}_s^3 - \lambda_\pi^2 \rho_\pi \bar{\sigma}_s - \frac{B_m}{\sqrt{2}} m_s\right].$$

$\Longrightarrow$ For $\boldsymbol{\rho_\pi < 0}$ (i.e., $\boldsymbol{T > T_c^{(N_f)}}$), $\bar{\sigma}_s$ must be positive;
$\Longrightarrow$ $\lim_{\bar{\sigma}_2 \to +\infty} \bar{\sigma}_s = \frac{k}{\lambda_\pi'^2}$.

Defining $F(\bar{\sigma}_2) = (\frac{1}{2}\lambda_\pi^2 + \lambda_\pi'^2)\bar{\sigma}_2^3 + (\lambda_\pi'^2 \bar{\sigma}_s^2 - \lambda_\pi^2 \rho_\pi - 2k\bar{\sigma}_s)\bar{\sigma}_2 - B_m m_l$:

$$F(0) = -B_m m_l < 0 \quad \text{and} \quad \lim_{\bar{\sigma}_2 \to +\infty} F(\bar{\sigma}_2) = +\infty.$$

For continuity of $F(\bar{\sigma}_2)$, there must be a positive root of the function. This root corresponds to a **positive solution of the SP condition** ($\boldsymbol{\bar{\sigma}_2, \bar{\sigma}_s > 0}$) provided that:

$$(\lambda_\pi^2 + \lambda_\pi'^2)\frac{k^3}{\lambda_\pi'^6} - \lambda_\pi^2 \rho_\pi \frac{k}{\lambda_\pi'^2} - \frac{B_m m_s}{\sqrt{2}} \neq 0.$$

Predictions of the model: meson mass spectrum

The fields η_l, η_h, σ_l and σ_h are the new **isospin singlet fields** that diagonalize the **squared mass matrix**:

$$\begin{cases} \eta_l \equiv \cos\theta_\eta \eta_2 - \sin\theta_\eta \eta_s \\ \eta_h \equiv \sin\theta_\eta \eta_2 + \cos\theta_\eta \eta_s \end{cases} \qquad \begin{cases} \sigma_l \equiv \cos\theta_\sigma \sigma_2 - \sin\theta_\sigma \sigma_s \\ \sigma_h \equiv \sin\theta_\sigma \sigma_2 + \cos\theta_\sigma \sigma_s \end{cases},$$

with

$$\sin 2\theta_\eta = \frac{2k\bar{\sigma}_2}{\sqrt{\left(\frac{\lambda_\pi^2}{2}\left(\frac{\bar{\sigma}_2^2}{2} - \bar{\sigma}_s^2\right) + k\bar{\sigma}_s\right)^2 + 4k^2\bar{\sigma}_2^2}};$$

$$\sin 2\theta_\sigma = \frac{2\bar{\sigma}_2(\lambda_\pi'^2\bar{\sigma}_s - k)}{\sqrt{\left[\frac{3\lambda_\pi^2}{2}\left(\frac{\bar{\sigma}_2^2}{2} - \bar{\sigma}_s^2\right) + \lambda_\pi'^2(\bar{\sigma}_2^2 - \bar{\sigma}_s^2) + k\bar{\sigma}_s\right]^2 + 4\bar{\sigma}_2^2(\lambda_\pi'^2\bar{\sigma}_s - k)^2}}.$$

Predictions of the model: minimum condition

For this solution to be a **point of minimum**, the mass spectrum must be always non-negative. To prove so, we rewrite the SP conditions:

$$\begin{cases} M^2_{\eta_s}\bar{\sigma}_s - \frac{B_m}{\sqrt{2}}m_s - k\bar{\sigma}_2^2 = 0 \\ M^2_\pi \bar{\sigma}_2 - B_m m_l = 0 \end{cases} \Longrightarrow M^2_\pi > 0 \iff \bar{\sigma}_2 > 0.$$

If we look at the pseudoscalar singlets block $\mathcal{M}^2_\eta = \begin{bmatrix} M^2_{\eta_2} & 2k\bar{\sigma}_2 \\ 2k\bar{\sigma}_2 & M^2_{\eta_s} \end{bmatrix}$:

$$\begin{cases} \mathrm{Tr}\mathcal{M}^2_\eta = M^2_{\eta_s} + M^2_\pi + 4k\bar{\sigma}_s > 0 \\ \det \mathcal{M}^2_\eta = M^2_{\eta_s} M^2_\pi + 2\sqrt{2}kB_m m_s > 0 \end{cases} \Longrightarrow M^2_{\eta_h} > M^2_{\eta_l} > 0.$$

Moreover, for every value of the parameters (and the vevs):

$$M^2_K \geq \min\left(M^2_\pi, M^2_{\eta_l}\right) > 0; \qquad M^2_\delta > M^2_\pi > 0;$$
$$M^2_\kappa > M^2_\pi > 0; \qquad M^2_{\sigma_h} > M^2_\pi > 0.$$

Predictions of the model: minimum condition

$\Longrightarrow$ The solution is in a minimum of the potential $\Longleftrightarrow$ $\det \mathcal{M}^2_\sigma > 0$

$$\det \mathcal{M}^2_\sigma = (2M^2_\pi - M^2_\delta)M^2_{\eta_s} + 2(\lambda^2_\pi + \lambda'^2_\pi)\left(\bar{\sigma}^2_2 M^2_{\eta_s} + \bar{\sigma}^2_s M^2_\pi\right) + 2\lambda^2_\pi(\lambda^2_\pi + 3\lambda'^2_\pi)\bar{\sigma}^2_2\bar{\sigma}^2_s + 8\lambda'^2_\pi\bar{\sigma}^2_2 k\bar{\sigma}_s + 2\sqrt{2}kB_m m_s.$$

This is positive whenever is met the **sufficient condition**:

$$\sqrt{2}M_\pi - M_\delta > 0.$$

Considering the data from [Bazavov et al., 2019b], this is verified above $T_{pc} = 156.5 \pm 1.5$ Mev.

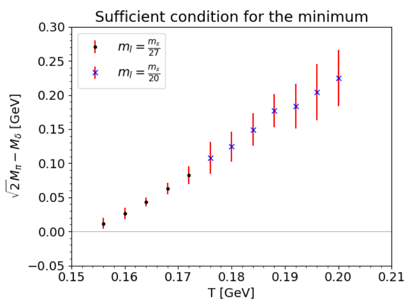

Figure 10: Sufficient condition for our solution to minimize the potential.

Comparison with the lattice data: $\frac{k^2}{\lambda_\pi^2}$

$$\frac{k^2}{\lambda_\pi^2} = \frac{1}{8}\frac{1}{(m')^2-1}\frac{(m'\Delta_{\delta\pi}-\Delta_{\kappa K})^2}{m'\Delta_{\kappa K}-\Delta_{\delta\pi}}.$$

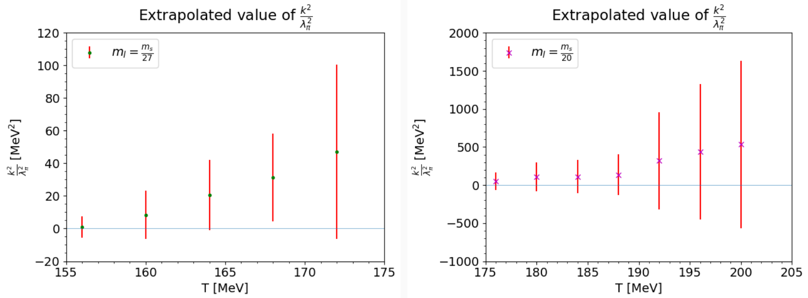

Figure 11: Extrapolated value of $\frac{k^2}{\lambda_\pi^2}$

$$kB_m m_l = M_\pi^2 k\bar{\sigma}_2.$$

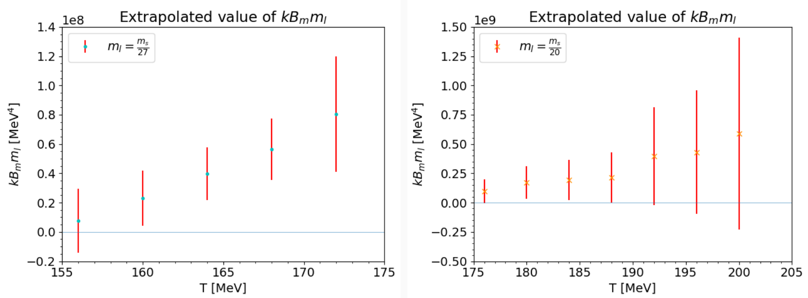

Figure 12: Extrapolated value of $kB_m m_l$.

Comparison with the lattice data: $-\lambda_\pi^2 \tilde{\rho}_\pi$

$$-\lambda_\pi^2 \tilde{\rho}_\pi = \frac{1}{2} \frac{(m')^2 + 1}{(m')^2 - 1} \left(M_\pi^2 + M_\delta^2 \right) - \frac{M_K^2 + M_\kappa^2}{(m')^2 - 1}.$$

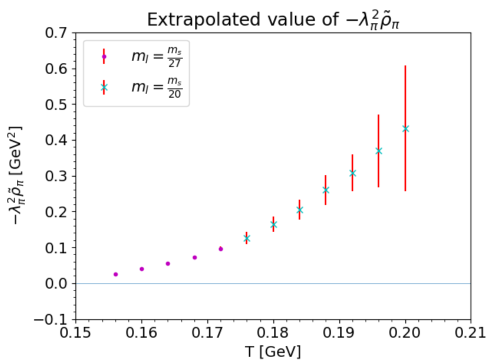

Figure 13: Extrapolated value of $-\lambda_\pi^2 \tilde{\rho}_\pi$.

Comparison with the lattice data: $-k^2\tilde{\rho}_\pi$

$$-k^2\tilde{\rho}_\pi = \frac{((m')^2+1)}{16((m')^2-1)^2}\frac{(M_\pi^2+M_\delta^2)-2(M_K^2+M_\kappa^2)}{M_K^2+M_\kappa^2-(M_\pi^2+M_\delta^2)}(m'\Delta_{\delta\pi}-\Delta_{\kappa K})^2.$$

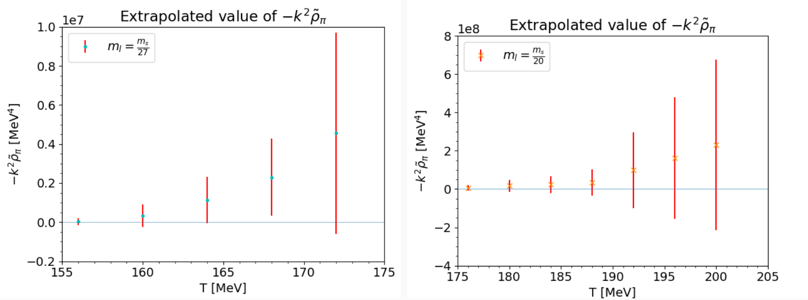

Figure 14: Extrapolated value of $-k^2\tilde{\rho}_\pi$

Comparison with the lattice data: pseudoscalar singlets

A further relation connects the **pseudoscalar singlet masses** (η_l, η_h) to those of pions and kaons:

$$
\begin{aligned}
M^2_{\eta_l,\eta_h} =& M^2_\pi + \frac{1}{4}((m')^2 - 1)\frac{\Delta_{\kappa K}}{m'} + \sqrt{2}\Big((m')^2 + \frac{1}{2}\Big)\frac{k\bar{\sigma}_2}{m'} \\
& \mp \sqrt{\Big[\frac{1}{4}((m')^2 - 1)\frac{\Delta_{\kappa K}}{m'} - \sqrt{2}\Big((m')^2 - \frac{1}{2}\Big)\frac{k\bar{\sigma}_2}{m'}\Big]^2 + 4k^2\bar{\sigma}_2^2}.
\end{aligned}
$$

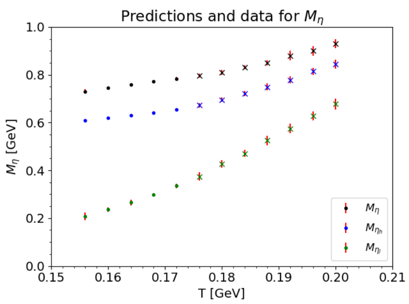

Figure 15: Predictions and data for M_η. Points correspond to $m_l = \frac{m_s}{27}$, while crosses to $m_l = \frac{m_s}{20}$.